NADH Regeneration Promoted by Solar Light Using Gold Nanoparticles/Layered Double Hydroxides as Novel Photocatalytic Nanoplatforms

Article *in* ChemistrySelect · October 2021

DOI: 10.1002/slct.202102221

4 authors, including:

Grosu Elena-Florentina
Gheorghe Asachi Technical University of Iasi
12 PUBLICATIONS **138** CITATIONS
SEE PROFILE

Renato Froidevaux
Université de Lille
63 PUBLICATIONS **767** CITATIONS
SEE PROFILE

Catalysis

NADH Regeneration Promoted by Solar Light Using Gold Nanoparticles/Layered Double Hydroxides as Novel Photocatalytic Nanoplatforms

Elena-Florentina Grosu,[a, b] Jean-Sébastien Girardon,[c] Gabriela Carja,[b] and Renato Froidevaux*[a]

Nicotinamide adenine dinucleotide NAD(P)H is a prolific cofactor in oxidoreductases biochemistry, but its high cost and the stoichiometric amounts motivates significant research for establishing efficient solutions for regenerating NAD(P)H from $NAD(P)^+$. This study presents nanoparticles of gold/layered double hydroxides (AuNPs/LDH) as nanoplatforms with highly efficient photocatalytic response for solar-light promoted NADH regeneration. The novel photocatalysts are obtained via self-assembling of ZnAlLDH and AuNPs by using the manifestation of the "structural memory" of the anionic clay in gold salt solution. The chemical composition, structural, optical and nanotextural features of AuNPs/LDH have been assessed by transmission electron microscopy (TEM), energy dispersive X-Ray Spectroscopy (EDX), powder X-ray diffraction (XRD), and UV-Vis Spectroscopy (UV-Vis). It was found that, at pH 8 and in the presence of flavin mononucleotide (FMN) as a mediator and using water as an electron donor, the regeneration the NADH under solar light is defined by a rate of 20.5 μM/h. Furthermore, the regenerated NADH cofactor is tested in presence of Horseradish Peroxidase (HRP) enzyme to promote the hydrogen peroxide reduction.

1. Introduction

The implication of enzyme catalysis for our word is tremendous. Enzymes act as catalysts and are involved in almost all the reactions which support life as digestion, respiration, photosynthesis, muscular contraction and other biological processes.[1] They are highly specific and can operate under mild conditions of pressure and temperature. Since their isolation, purification and characterization were possible, the enzymes started to gain interest as excellent eco-friendly catalysts for the industrial chemicals production.[2,3]

Oxidoreductases are a large group of enzymes, that are attractive biocatalysts for the synthesis of valuable chemicals and pharmaceutical products,[4] however they must be used with complex and expensive cofactors such as nicotinamide adenine dinucleotide (NADH) or with its phosphorylated correspondent (NADPH). During the enzymatic reaction, cofactors are reduced or oxidized, while the enzyme remains unmodified. Since the enzyme catalyzes continuously the same process, the cofactor has to be always available in the system, thus their cost efficient regeneration processes are important.[5]

NADH acts as hydrogen donor and leads to NAD^+ formation. Because of high NADH price (approximatively 2600 $/mol), its regeneration by NAD^+ reduction is the most adequate option.[6] In living cells, the conversion of cofactor from the reduced to oxidized one and reverse is carried out by a network of enzymatic reactions.[5] On the other hand, in situ regeneration process involves the use of secondary substrate and enzyme able to convert the $NAD(P)^+$ to NAD(P)H or vice versa.[4] Despite their high selectivity for the active NAD(P)H, the enzyme-based cofactor regeneration in industrial processes is not economically viable, because of the expensive enzymes price.[7] Furthermore, the process effectiveness is limited by the production of a significant amount of byproducts, whose separation is also costly. Even so, because the lack of suitable solutions, at the industrial level, the cofactors have been regenerated only via enzymatic pathway. However, aspects as enzyme instability and deactivation, the need of supplementary reactants for maintaining the optimal enzyme operational conditions, as well as the complexity of product purification, highlight the necessity of finding new methods for cofactor regeneration.[4] Whole-cells NADH regeneration comes as an extent for the enzymatic route, but **without the enzyme purification steps**. When cofactors are regenerated via whole–cell pathway, the control of the primary and auxiliary enzyme production is difficult to be achieved.[8] Furthermore, cells contain more than one type of enzymes, so side reactions can take place.[4] Medium contamination with different components

[a] *Dr. E.-F. Grosu, Prof. R. Froidevaux*
EA7394-ICV-Institut Charles Viollette
UMR Transfrontalière 1158 BioEcoAgro, Univ. Lille, INRAE, Univ. Liège, UPJV, JUNIA, Univ. Artois, Univ. Littoral Côte d'Opale, ICV-Institut Charles Viollette, F-59000 Lille, France
E-mail: renato.froidevaux@univ-lille.fr
[b] *Dr. E.-F. Grosu, Prof. G. Carja*
Department of Chemical Engineering
Gheorghe Asachi Technical University
Bul. Profesor Dimitrie Mangeron 73, Iasi 700554, Romania
[c] *Dr. J.-S. Girardon*
UMR 8181-UCCS-Unité de Catalyse et Chimie du Solide
Lille University, CNRS, Centrale Lille, ENSCL, Artois University
Avenue Paul Langevin, 59655 Villeneuve d'Ascq Cedex, France

Supporting information for this article is available on the WWW under https://doi.org/10.1002/slct.202102221

of the cell can also occur.[9] Additionally, in order to facilitate the substrate transport through cell membrane, organic detergents have been used to increase permeabilization.[10] Promising results were obtained with **cell surface-displayed enzymes**. This type of systems are able to solve enzyme stability problems and the mass transfer limitations.[11] The major barrier in **surface display technology to industrial application is the low enzyme concentration in the cell wall.**[9] Besides the enzymatic route, a broad range of non-enzymatic NAD^+ reduction methods have been developed to overcome the shortcoming of the traditional regeneration way.[4,12]

The non-enzymatic cofactor regeneration by using catalytic, electrochemical or photochemical reactions can be associated with advantages as cleanliness, process simplicity and the use of cheap, clean and renewable energy. Nevertheless, comparing with the enzymatic route, some of these methods are mediator dependent, and in some situations, the selectivity might be also an issue.[7] In terms of NADH regeneration, these techniques presented good cofactor conversion yields, but the regeneration rates are much higher in case of photocatalytic reactions, compared, for instance with the electrocatalytic one.[4,13] Furthermore, finding an efficient mediator with high selectivity for the active NADH isomer is a good strategy to overcome the selectivity problems. Results have proven that the mediators as flavin mononucleotide (FMN) and $[Cp^*Rh(bpy)H_2O]^{2+}$ **were selective toward 1,4-NADH photoconversion.**[14,15]

The irradiation, in special the solar one, is a low cost and clean energy source. The natural reduction of NAD^+ to NADH initiated by the solar light during photosynthesis, inspired the photocatalytic regeneration of cofactors using simulated irradiation. Efforts have been focused in designing photoreactors as valuable tools in performing accurate and reproducible processes.[16,17] On the other hand, promising results were obtained also for photocatalytic reactions initiated directly by the natural sun irradiation.[18–20] Considering cofactor regeneration, by now, the most prospected catalyst is TiO_2.[14,21,22] Generally, a photocatalytic system designed for cofactor regeneration contains a catalyst, an electron donor (**triethanolamine – TEOA**, **ethylenediaminetetraacetic acid – EDTA, ascorbic acid**) and a mediator (**flavin mononucleotide – FMN**, $[Cp^*Rh(bpy)H_2O]^{2+}$), which facilitates the charge transfer.[14,23,24] Recently, K.A. Brown et al.[24] efficiently succeed in the regeneration of NADPH by using visible light and a combination between CdSe quantum dots and ferredoxin $NADP^+$-reductase. Heterogeneous Pt based catalysts were as well investigated and permitted a conversion of more than 50% of the initial NAD^+ concentration.[4,25] Additionally, organic semiconductors as g-C_3N_4, in presence of $[Cp^*Rh(bpy)H_2O]^{2+}$ and TEOA as a mediator and electron donor, are good alternatives to photoreduce the NAD^+ in a range of 50 to 100%.[26–29]

In order to decrease the process costs and also to limit the generation of additional wastes, Mifsud et al.[14] highlighted that water molecule can behave as sacrificial electron donor, driving biocatalytic redox processes with TiO_2 based catalysts, under light irradiation. Similar observation was obtained in works of Aresta et al.[15] Those authors showed that a NADH photoregeneration can be initiated by a wide range of solid catalysts by using water as an electron donor.

Noble elements as Pt, Ag and Au nanoparticles (NPs) exhibit unique and versatile plasmonic properties allowing them to be used in light driven reactions. Despite their high potential in photocatalysis, the traditional synthesis methods for this kind of nanoparticles involve the use of organic compounds,[30] sometimes costly and environmentally-unfriendly. Doping different semiconductor materials with nanoparticles comes as an efficient way to obtain composites with improved photocatalytic properties.[31–34] Recently, we report a simple way to synthetize AuNPs self-assembled on layered double hydroxide (LDH) semiconductors, by using the unique property of these anionic clays to re-build their lamellar structure after thermal treatment. Furthermore, without using any **organic surfactants and/or stabilizers for NPs**, the results show that gold nanoparticles can interact intimately with the LDH matrix, leading to a highly preformat photocatalyst for organic pollutants solar photodegradation.[35] Moreover, the presence of the plasmonic NPs on semiconductor photocatalysts can increase the life time of the photo induced charge carriers, and the photocatalytic performance is enhanced.[36]

The LDH-2D materials, with their characteristics as high surface area, ionic exchange capacity, semiconductor properties and easy tunable textural and morphological features, are used many times in processes initiated by light.[37–40] However, as far as we know, no work deals with their potential application to regenerate the NADH from NAD^+. Since AuNPs,[41] PtNPs[4,25] were successfully used for cofactors regeneration, the aim of this work is to be a proof of concept for the ability of supported AuNPs on ZnAl-LDH catalysts to photo-initiate the NAD^+ reduction reaction. The photocatalytic regeneration is driven under solar simulated light, using water as a sacrificial electron donor and flavin mononucleotide (FMN) as a mediator.

2. Results and Discussions

2.1. Materials characterization

In Table 1 is listed the elementary analysis using EDX. The obtained values are regular with the hydrotalcite structure.[42] After reconstruction, the presence of Au phase is also confirmed.

The optical properties before and after AuNPs formation on the LDH surface are shown in Figure 1A. The absorption peak at 560 nm appears due to AuNPs surface plasmon resonance (SPR). According to previous data, for this SPR response, the dispersed AuNPs on LDHs matrix have particles size around 10–15 nm.[35,43,44] The XRD pattern corresponding to ZnAl-LDH

Table 1. Chemical composition of the catalysts according to EDX data.

Sample	% O	% Al	% Zn	% Au
ZnAl-LDH	54	10	36	0
AuNPs/ZnAl-LDH	54.75	8.25	28	5.125

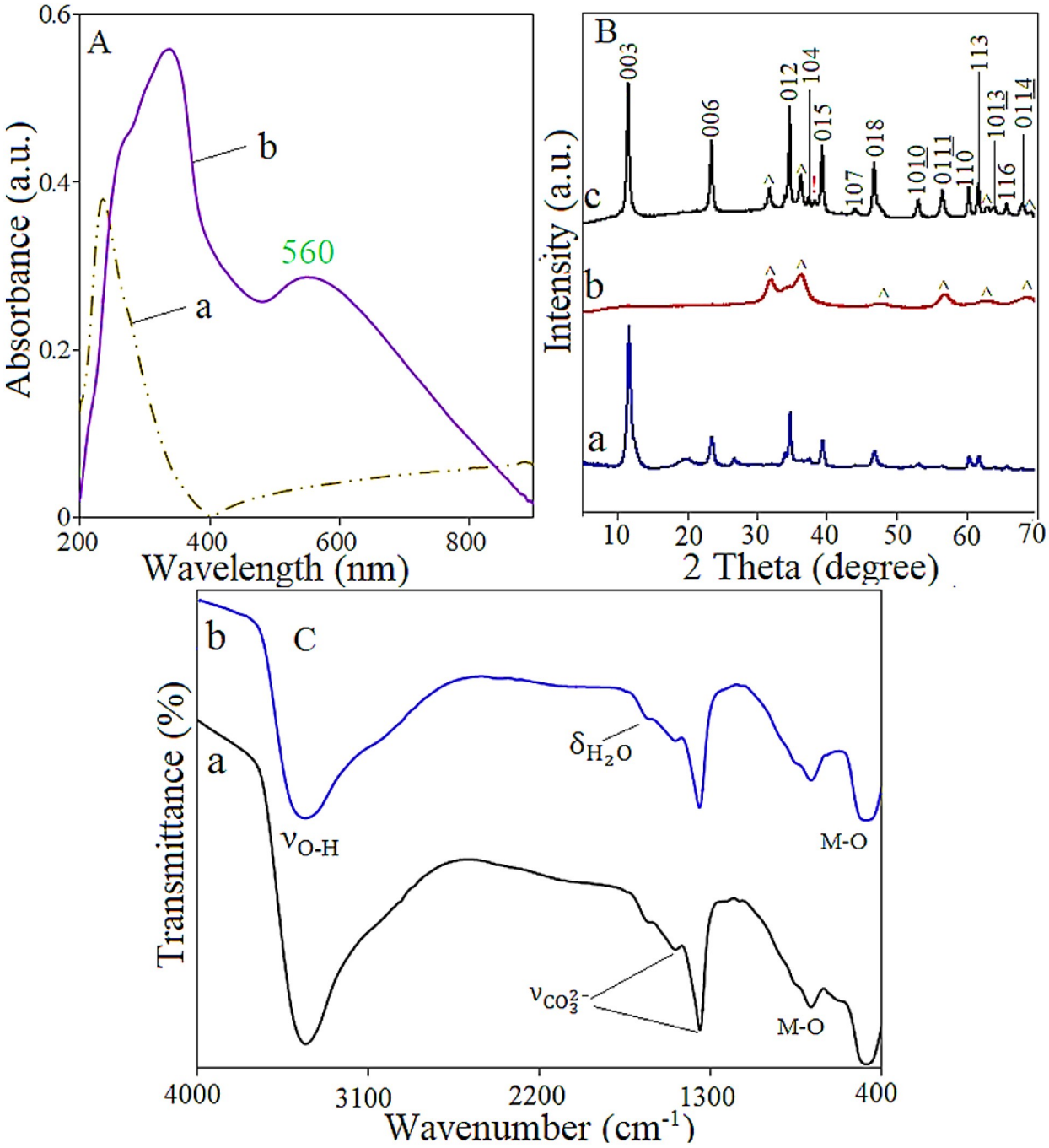

Figure 1. A) UV-Vis spectra for a) ZnAl-LDH, b) AuNPs/ZnAl-LDH; B) XRD patterns for a) ZnAl-LDH, b) ZnAl-525, c) AuNPs/ZnAl-LDH; ( ) ZnO; (!) AuNPs; C) FTIR spectra of a) ZnAl-LDH, b) AuNPs/ZnAl-LDH.

support (Figure 1B) confirms a typical hydrotalcite structure characterized by the diffraction peaks at 2Θ = 11.7, 23.5, 34.6, 37.4, 39.3, 44.04, 46.8, 52.9, 56.5, 60.3, 61.5, 63.7, 65.8, 67.8 ° attributed to (003),(006), (012), (104), (015), (107), (018), (10$\underline{1}$0), (01$\underline{1}$1), (110), (113), (10$\underline{1}$3), (116), (01$\underline{1}$4) diffraction planes.[45] After the thermal treatment at 525 °C, the initial LDH structure collapses and the ZnO phase with characteristic peaks at 31.8, 36.2, 47.9, 56.7, 62.9, 68.1° assigned to (100), (101), (102), (110), (103) and (112) reflection planes is formed.[46] It is remarkable than after gold self-assembly, the XRD profile of the catalyst indicates, besides the usual hydrotalcite structure signals, apparition of peaks at 2Θ = 31.6 and 36.2 assigned to the (010) and (011) diffraction planes highlighting the presence of ZnO crystalline phase.[47] The AuNPs are confirmed by a diffraction peak at 2Θ = 38.1 attributed to (111) standard Bragg reflections plans.[48] The lattice parameters ($a = 2d_{110}$ and $3c = 3d_{003}$) and

the crystal size, calculated with Scherrer equation, are given in Table 2. The values of $d_{003} = 0.75$ nm for ZnAl-LDH support and 0.76 nm for AuNPs/ZnAl-LDH catalyst seems to confirm that the interlayer anion is CO_3^{2-}. The "a" cell parameter, which gives information about the cation-cation distance in the brucite layer,[49] remains constant after gold deposition. Further, the FTIR analysis was performed to confirm the nature of functional groups from the LDH samples and the nature of the interlayer anions. The FTIR spectra are presented in Figure 1C. The vibrations bands around 3450 cm^{-1} are assigned to O–H stretching of the lamella hydroxyl groups, the interlayer water which is characterized by a shoulder at 1637 cm^{-1} and the interlayer anion, CO_3^{2-}, with a weak intensity band at 1490 cm^{-1} and an intense one at 1360 cm^{-1} confirm that the synthetized materials have LDH structure.[49]

The thermal stability of ZnAlLDH was investigated in a temperature range between 30 −800 °C. The TG/DTG and TG/DTA are listed in Figure 2. The composite presents three major weight loss steps. The first event, assigned to the surface and interlayer water removal, takes place between 40–200 °C. An increase of temperature up to 280 °C leads to the layers dehydroxylation. The mass loss between 280–500 °C is assigned to the interlayer anion decomposition.[50] A small decrease of weight takes place also in the interval 500–800 °C, and is attributed to the removal of the strongly adsorbed carbonate anions on the formed mixed oxides.[51] These mass losses are supported by the DTG curve which presents an edge at 100 °C and three endothermic peaks at 200 °C, 274 °C and 580 °C. The peak around 580 °C is an evidence that the initial LDH structure collapsed and metal oxides phase was formed.[39] The same processes are confirmed also by DTA via a peak at 204 °C and two edges at 112 °C and 280 °C, corresponding to endothermic transformations as water removal, lamella dehydroxylation and carbonate anions decomposition.

Representative TEM, HRTEM images and SAED patterns assigned to the obtained materials are displayed in Figure 3. The TEM picture 3a of the ZnAl-LDH support shows large plates, which overlap, representing the typical hydrotalcite morphology.[52] After self-assembly of gold, homogeneously dispersed spherical AuNPs with diameters between 7–20 nm are observed on the support (Figure 3b, 3c). These observations are in good agreement with previous researches revealing that this kind of materials, synthetized under similar conditions, lead to 9–11 nm AuNPs size.[43] Few agglomerated AuNPs with diameters between 60–120 nm are also observed (Figure S1). As shown in picture 3d, the measured 0.24 nm interplanar spacing is characteristic to the {111} face centered cubic gold structure[53] and confirmed by the spacing attributed to (111), (200), (210) and (311) rings patterns in Figure 3e. Moreover, it was demonstrated that ZnO has not a separate morphology, but is embedded inside the LDHs matrix.[54]

Table 2. Crystal size and lattice parameters for the investigated materials.

Sample	Crystal size (nm)	a (Å)	c (Å)
ZnAl-LDH	15	3.062	22.5
AuNPs/ZnAl-LDH	18	3.067	22.8

2.2. NADH photocatalytic regeneration

The LDH materials are able to adsorb molecules to a certain extent, in function of their characteristics. In photocatalysis, the adsorption of the specific compounds on the LDH surface plays a crucial role, because the photocatalytic reactions take place predominantly on the surface of the photocatalyst.[55] For this reason, before starting any photocatalytic experiments, the reactants and the nanocomposite were stirred in the dark for 30 minutes. Samples were taken once at ten minutes and the extent of adsorption on the material surface was monitored by

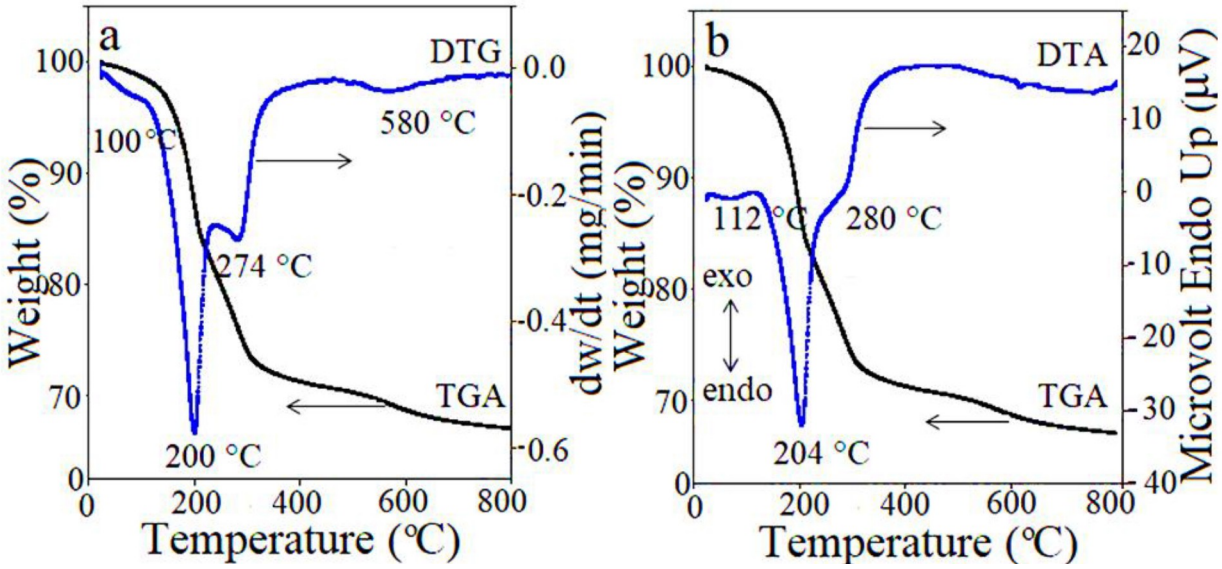

Figure 2. a) TGA/DTG and b) TGA/DTA for ZnAl-LDH.

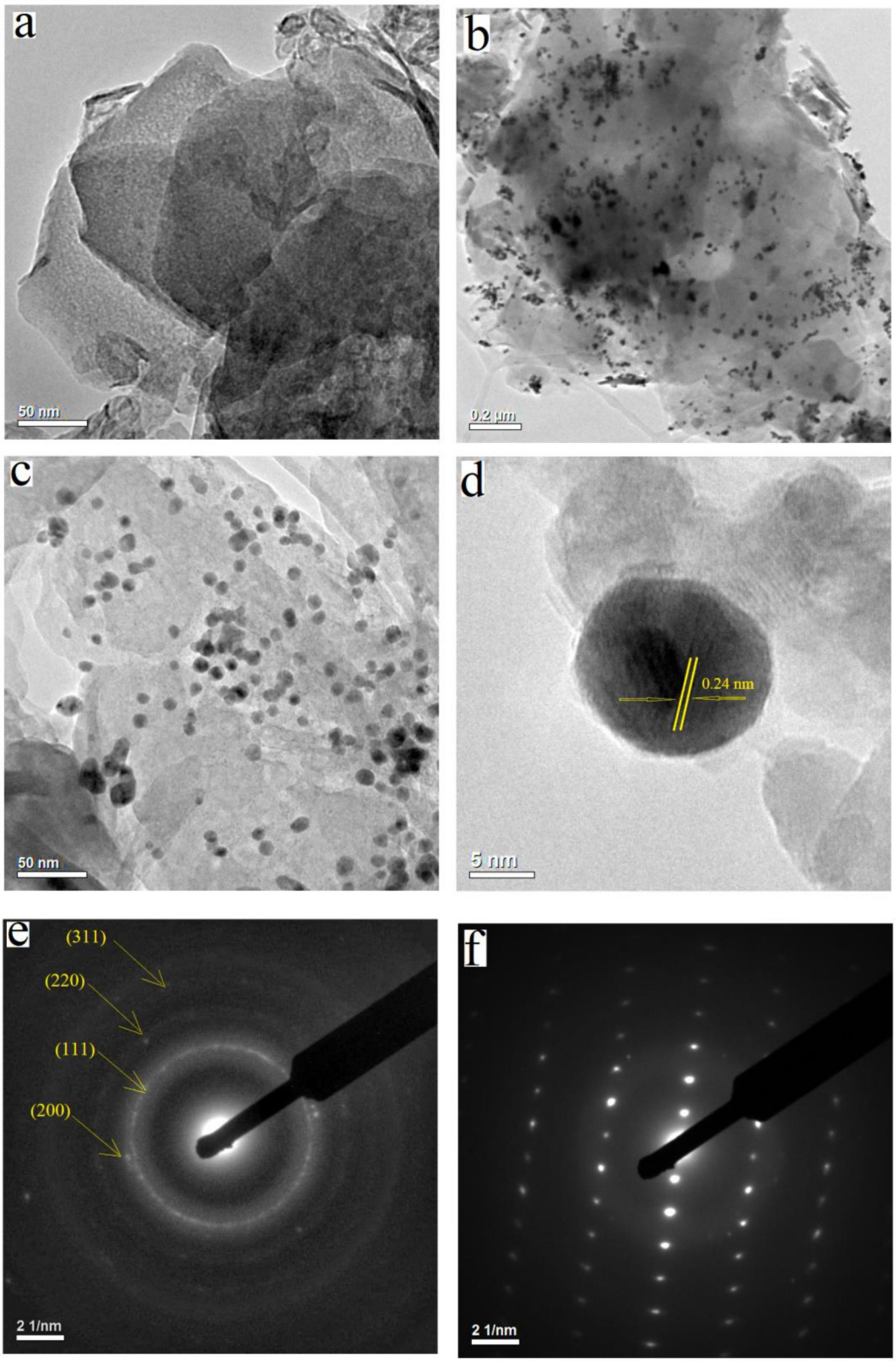

Figure 3. TEM images for a) ZnAl-LDH, b-c) AuNPs/ZnAl-LDH, d) HRTEM image of AuNPs/ZnAl-LDH, and e–f) SAED patterns of AuNPs/ZnAl-LDH.

recording the UV-Vis spectra of the centrifuged solutions. In Figure S2 can be observed that the adsorption-desorption equilibrium was reached after 20 minutes. A significant adsorption of NAD^+ and FMN was noticed for all pH values. It

seems that the pH decrease favors a slightly increase of the adsorption capacity.[56] The NADH adsorption on AuNPs/ZnAl-LDH was also approached (Figure S2d). The adsorption-desorption equilibrium was reached after 20 minutes, but the yield was less significant compared with that of NAD^+ and FMN molecules. This might underline that the initial reactants present a stronger affinity for the nanocomposite surface than NADH. Furthermore, during the adsorption-desorption of NAD^+ and FMN mixture a saturation plateau was reached, so it can be assumed that during the product formation, no significant adsorption of NADH will take place.

The photocatalytic activity of LDH based catalyst is tested at room temperature, monitoring by UV-Vis spectroscopy the solar regeneration of NADH in presence of FMN as electron mediator and water as an electron donor.[57–62] The pH solution is a strong parameter for the cofactor regeneration efficiency, thus 3 tests are performed at pH = 6, 7 and 8. All recorded UV-Vis spectra are reported in Figure 4. Figure 4a presents references spectra of the alone molecules and in mixtures, but without presence of LDH. It is remarkable that the absorption peak at 260 nm is not the recommended peak for molecules discrimination, since it is common to all. Figures 4b, 4c, 4d, present the UV-Vis spectra obtained for the test solutions in presence of AuNPs/ZnAl-LDH, as a function of illumination time. In all pH conditions, an absorption peak appears at 340 nm and grows progressively. This signal is attributed to the NADH formation. Pending two hours of irradiation, the peak absorbance increases. An increase of the absorbance placed at 260 nm is also noticed. Even if NADH and NAD^+ have a common signature peak at this wavelength, the increase of the absorbance peak at 260 nm with irradiation time could suggest a product generation, and can be attributed to NADH formation. HPLC analyze (High Performance Liquid Chromatography) for the regenerated cofactor was also performed. In

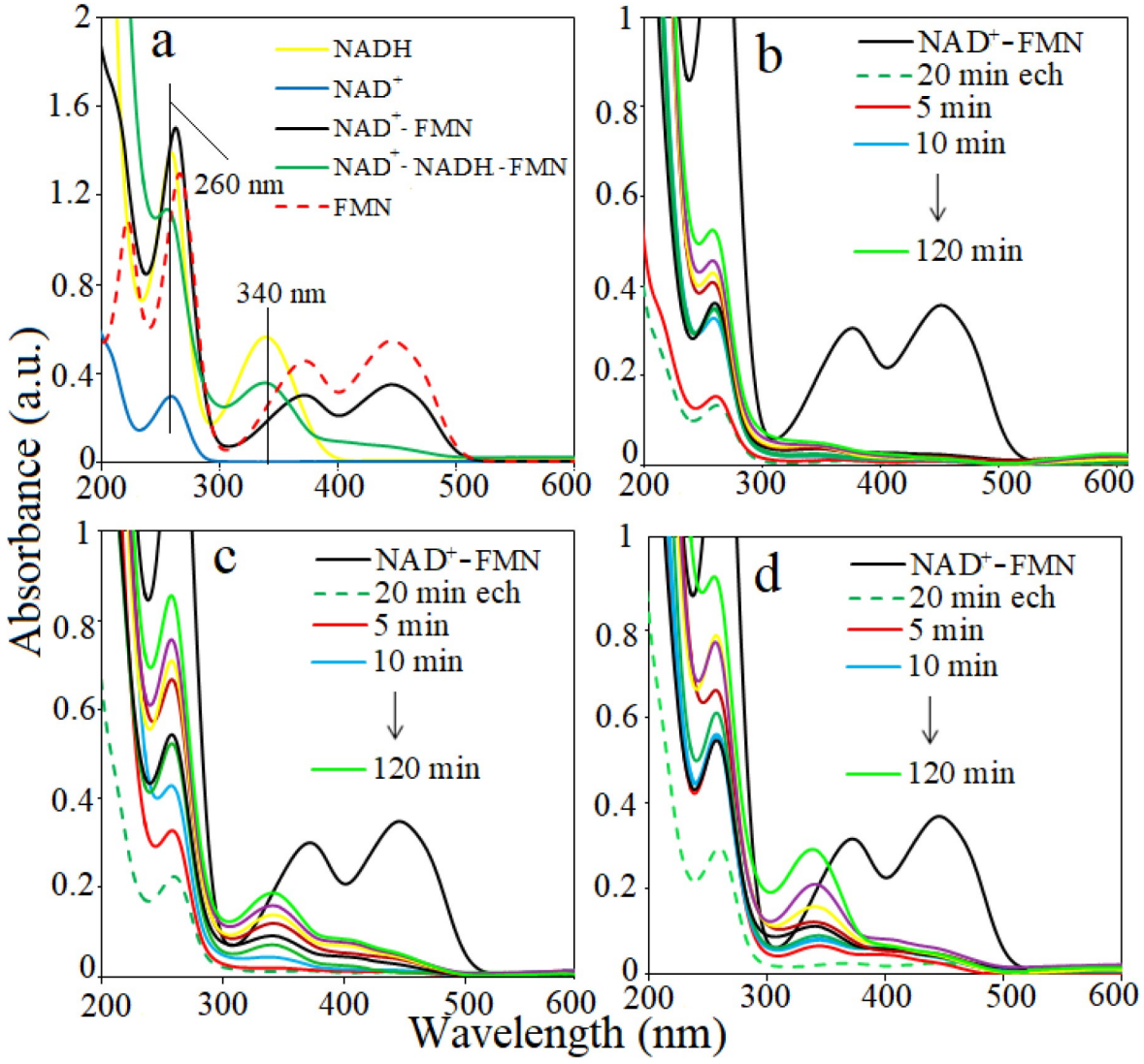

Figure 4. a) UV-Vis spectra for fresh standard solutions of NAD^+, FMN, NADH, NADH-NAD^+-FMN and NAD^+-FMN; UV-Vis spectra profiles for the NADH regeneration for b) pH 6, c) pH 7 and d) pH 8; *20 min ech* is the UV-Vis spectra of the NAD^+-FMN after 20 minutes of equilibrium in the dark.

Figure S3 are presented the HPLC chromatograms for the NAD^+, FMN, FMN + NAD^+, NADH standards together with the photoregenerated NADH at 280 nm. It can be observed that the regenerated metabolite presents signals at retention times (3.63, 3.29, 3.14 minute) fitting with those of the standards, ±0.03–0.08 min, underlining the presence of NADH, but also of unreacted NAD^+.

The best-fit equation to describe the kinetic of NADH formation is a zero order reaction. The dependence between C_{NADH} (NADH concentration, μM) and *t* (time, min) is presented in Figure 5. Using a NADH standard curve, the cofactor regeneration yield was calculated. In Table 3 are listed the reaction constant, *k*, calculated on the basis of the lines slope together with the cofactor regeneration yield. According with these data, the maximum yield of NADH regeneration was reached at pH 8 (73%), while at pH 7, the conversion was 50%. When the hydrogen ions concentration increases, the NADH photocatalytic regeneration is significantly decelerated. In terms of reaction rate and pH influence over the regeneration process, our results are in good agreement with those reported by.[25,63] Studies on the same topic have revealed that the optimal pH for the NADH regeneration can be different in function of the catalyst characteristics. However, promising results were obtained in a range of pH between 7–9.[25,26,64]

Some control tests were also performed, as follows: NAD^+ + FMN + hν; NAD^+ + Au/ZnAl-LDH + hν; ZnAl-LDH + NAD^+ + FMN + hν. It was remarked that the presence of the AuNPs/ZnAl-LDH, light and FMN electron mediator are mandatory for the NAD^+ reduction. Furthermore, the test carried out by replacing the AuNPs/ZnAl-LDH with the parent material, ZnAl-LDH, had no performance for the photoconversion of the cofactor, underlining that the AuNPs are responsible for the photoregeneration. The quantity of ZnO phase in the catalyst is very small and it can not decisively alter the catalytic activity.[35,65] Moreover, for the NADH photoregeneration, ZnO was reported to be inactive.[27]

Our results are comparable with the one obtained in other studies dealing with NADH photoregeneration.[22,25,64] However, our system had a superior performance compared with the doped or the simple TiO_2, when even if in presence of a mediator, the cofactor was poorly regenerated.[15] Organic semiconductors, as g-C_3N_4 was able to regenerate up to 100% of NADH in presence of electron donor and mediator.[26] In Table 4 are given other results obtained by different researchers when NADH was photocatalytically regenerated. It can be observed that the catalysts are more complex and their fabrication involved several organic agents compared with the one we obtained.

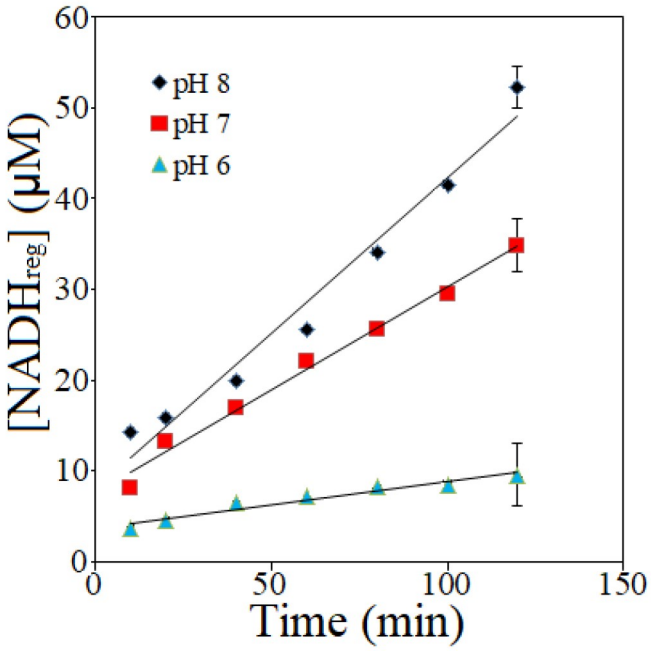

Figure 5. Kinetic plot of photochemical NADH production using AuNPs/ZnAl-LDH.

Table 3. Kinetic results/yield for the NADH photoregeneration process after 2 h of solar irradiation.

Kinetic results/yield	pH 8	pH 7	pH 6
k, μM/h	20.5	13.6	3
$NADH_{reg}$ (%)	73	50	14

A mechanism for the NADH regeneration, using solar light and AuNPs/ZnAl-LDH nanocomposite is proposed in Figure 6. Under solar irradiation, electrons-hole pairs are formed as a result of catalyst interaction with light. The irradiation induces an electron transfer from the valence band to conduction

Table 4. Comparison of different solid photocatalysts used in NADH photoregeneration.

Photocatalyst	Dose	Irradiation source	NAD^+ initial	NADH regen.,%	Ref.
Pt coated AuNPs	111 μM	400–1200 nm, 150 mW/cm^2	1 mM	10 in 2 h	[66]
CCGCMAQSP – graphene based catalyst	0.161 mg/L	450 W Xenon lamp, >420 nm	400 μM	46 in 2 h	[67]
$W_2Fe_4Ta_2O_{17}$	0.161 mg/mL	450 W Xenon lamp, >420 nm	400 μM	15 in 2 h	[67]
Carbon-TiO_2	Not given	8 W lamp, >400 nm	0.2 mM	50 in 10 h	[22]
PtNPs	370 μM	330 W Xenon lamp, >420 nm	0.2 mM	86 in 12 h	[63]
CdS-SiO_2	Not given	>420 nm	1 mM	80 in 1 h	[68]
PHTT_DMP polymer	0.2 mg/mL	MI-150TM, 150 W, >420 nm	1 mM	10 in 2 h	[69]
P-doped TiO_2	0.8 mg/mL	8 W lamp, >400 nm	0.2 mM	35 in 9 h	[70]
g-C_3N_4-@α-Fe_2O_3/C	0.5 mg/mL	100 W LED, 405 nm	1 mM	76 in 16 min	[71]
Graphene-BODIPY	0.161 mg/mL	450 W Xenon lamp, >420 nm	400 μM	54 in 2 h	[72]
AuNPs/ZnAl-LDH	1 mg/mL	180 W solar lamp	70 μM	73 in 2 h	This study

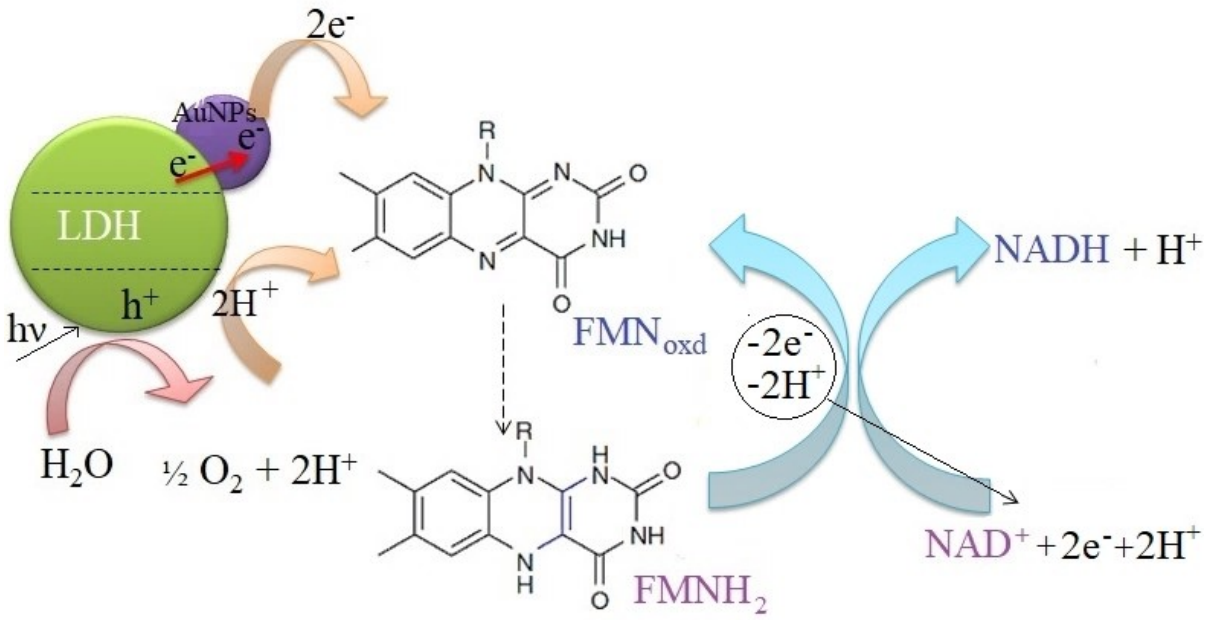

Figure 6. The proposed mechanism for the solar photoregeneration of NADH by using AuNPs/ZnAl-LDH catalyst.

band. The holes (h^+) from the valence band will form oxidizing species as a result of water oxidation, while the electrons (e^-) from the LDH conduction band will be trapped by the AuNPs which are intimately contacted with the LDH surface.[36] Then, the electrons can move freely at the nanoparticles surface and together with the generated H^+ species will participate to the reduction reaction of the FMN_{ox}. In presence of NAD^+, the $FMNH_2$ will be oxidized, while the NAD^+ will be converted in NADH.[14]

The NADH cofactor has three isomers: 1,4 NADH, which is enzymatically active, and its inactive 1,2 NADH and 1,6 NADH forms.[6] When the cofactor is regenerated via an alternative method, it is important to know if the obtained isomer is 1,4 NADH, the enzymatically active form. According to the studies presented by Chen and Rocha-Martin,[73,74] peroxidases can mediate redox reactions as the H_2O_2 reduction or phenols oxidation by substrates as 1,4 NADH. For this reason, the photoregenerated cofactor was used to convert H_2O_2 to H_2O mediated by HRP as described by.[26] To 1 mL fresh regenerated NADH (pH 8), 60 U HRP, and 30 μL H_2O_2, 30% were added and incubated at room temperature. UV-Vis spectra were recorded at specific moments and they are presented in Figure 7. In presence of HRP and H_2O_2, the initial cofactor profile modifies. The peak at 340 nm is shifted to a shoulder shape, which decreased in time as a result of NADH consumption by H_2O_2 reduction mediated by the enzyme.[26] A control test was done by using commercial NADH. The reaction takes place in a similar way, while the reference NADH solutions, with only HRP or H_2O_2 presented also some difference in absorbance, but less significant (see Figure S4).

3. Conclusions

Results point out the simple fabrication of self-assembled nanoparticles of gold on layered double hydroxides matrix, and their utilization in NADH regeneration by solar-light induced photocatalysis. The synthesis is free of organic agents and it is carried out by exploring the structural memory property of

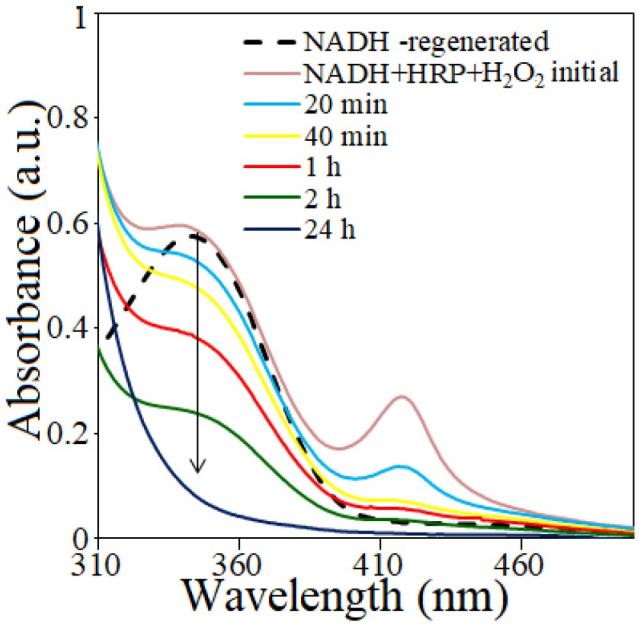

Figure 7. NADH absorbance profile changes during the HRP mediated H_2O_2 conversion into H_2O.

hydrotalcite materials. The materials characterization reveals that on the clay surface, spherical AuNPs with dimensions between 7–20 nm are dispersed. When tested, our nanocomposite exhibits outstanding photocatalytic activity for regeneration of NADH under solar light. The cofactor regeneration takes place in presence of FMN as an electron mediator and water is used as an electron donor. From the excited state of AuNPs, electrons with high levels of energy are transferred into the process and after two hours of solar irradiation, 73% of NAD^+ are converted in NADH. In presence of HRP, the regenerated cofactor participates at the conversion of H_2O_2 in H_2O, confirming that the active 1,4 NADH isomer is present in the product solution. To note that, this is the first study when LDH based nanocomposites are used to regenerate the NADH from NAD^+.

Supporting Information

The supporting information includes the experimental section, as well additional experimental data.

Acknowledgments

work was supported by the Alibiotech project which is financed by European Union, French State and the French Region of Hauts-de-France. The authors thank to Joelle Thuriot (REALCAT platform - BFuture Investments program (PIA), with the contractual reference ANR-11-EQPX-00370), Eric Gautron (Institut des Materiaux Jean Rouxel - NANTES -France), and Justine Dillies for their help in obtaining the XRD, TEM, EDX and HPLC data. FEDER is also acknowledged for supporting and funding partially this work.

Conflict of Interest

The authors declare no conflict of interest.

Keywords: gold · layered double hydroxide · nanoparticles · nicotinamide adenine dinucleotide · photocatalysis.

[1] J. B. Sumner, *J. Chem. Educ.* **1952**, *29*, 114.
[2] S. Shoda, H. Uyama, J. Kadokawa, S. Kimura, S. Kobayashi, *Chem. Rev.* **2016**, *116*, 2307.
[3] S. Dai, L. Xue, M. Zinn, Z. Li, *Biomacromolecules* **2009**, *10*, 3176.
[4] X. Wang, T. Saba, H. H. P. Yiu, R. F. Howe, J. A. Anderson, J. Shi, *Chem* **2017**, *2*, 621.
[5] V. Uppada, S. Bhaduri, S. B. Noronha, *Curr. Sci.* **2016**, *106*, 946.
[6] T. Saba, J. W. H. Burnett, J. Li, P. N. Kechagiopoulos, X. Wang, *Chem. Commun.* **2020**, *56*, 1231.
[7] H. Wu, C. Tian, X. Song, C. Liu, D. Yang, Z. Jiang, *Green Chem.* **2013**, *15*, 1773.
[8] E. Su, M. Yang, C. Ning, X. Ma, S. Deng, *J. Biotechnol.* **2018**, *271*, 1.
[9] M. Lozancic, A. S. Hossain, V. Mrša, T. Renata, *Catal. Rev.* **2019**, *9*, 728.
[10] L. Han, B. Liang, *World J. Microbiol. Biotechnol.* **2018**, *34*, 141.
[11] J. Schüürmanna, P. Quehl, F. Lindhorst, K. Lang, J. Jaachim, *Biotechnol. Bioeng.* **2017**, *114*, 1658.
[12] A. Weckbecker, H. Groger, H. Werner, in *Adv. Biochem. Eng. / Biotechnol.* (Eds: C. Wittmann, R. Krull), Springer Berlin Heidelberg, Berlin, **2010**, 195–242.
[13] R. Jayabalan, M. Sathishkumar, E. S. Jeong, S. P. Mun, S. E. Yun, *Bioresour. Technol.* **2012**, *123*, 686.
[14] M. Mifsud, S. Gargiulo, S. Iborra, I. W. C. E. Arends, F. Hollmann, A. Corma, *Nat. Commun.* **2014**, *5*, 3145.
[15] M. Aresta, A. Dibenedetto, T. Baran, A. Angelini, P. Łabuz, W. Macyk, *Beilstein J. Org. Chem.* **2014**, *10*, 2556.

[16] P. Mazierski, B. Bajorowicz, E. Grabowska, Z. Adriana, in *Heterog. Photocatal. From Fundam. to Green Appl.* (Eds: J. C. Colmenares, X.-J. Xu), Springer-Verlag Berlin Heidelberg 2016, Berlin, **2016**, 213–245.
[17] V. Nguyen, C. S. Wu, *Appl. Catal. A* **2018**, *550*, 122.
[18] Ritika, M. Kaur, A. Umar, S. K. Mehta, S. Singh, S. K. Kansal, H. Fouad, O. Y. Alothman, *Materials (Basel).* **2018**, *11*, 2254.
[19] Ritika, M. Kaur, A. Umar, S. Kumar, S. Kumar, *Mater. Res. Bull.* **2019**, *112*, 376.
[20] J. Park, I. Cho, Y. Kim, *J Env. Sci Heal. A Tox Hazard Subst Env. Eng.* **2004**, *A39*, 159.
[21] Y. Ho, A. P. Periasamy, S. Chen, *Sens. Actuators B* **2011**, *156*, 84.
[22] Z. Jiang, C. Lu, H. Wu, *Ind. Eng. Chem. Res.* **2005**, *44*, 4165.
[23] G. T. Höfler, E. Fernández-Fueyo, M. Pesic, S. H. Younes, E. Choi, Y. H. Kim, V. B. Urlacher, I. W. C. E. Arends, F. Hollmann, *ChemBioChem* **2018**, *19*, 2344.
[24] K. A. Brown, M. B. Wilker, M. Boehm, H. Hamby, G. Dukovic, P. W. King, *ACS Catal.* **2016**, *6*, 2201.
[25] J. H. Kim (Ewha University), South Korea, WO2011108789 A1, **2010**.
[26] J. Liu, M. Antonietti, *Energy Environ. Sci.* **2013**, *6*, 1486.
[27] J. Huang, M. Antonietti, L. Jian, *J. Mater. Chem. A* **2014**, *2*, 7686.
[28] X. Huang, H. Hao, Y. Liu, Y. Zhu, X. Zhang, *Micromachines* **2017**, *8*, 175.
[29] J. Liu, J. Huang, H. Zhou, M. Antonietti, *ACS Appl. Mater. Interfaces* **2014**, *6*, 8434.
[30] A. Loiseau, V. Asila, G. Boitel-Aullen, M. Lam, M. Salmain, S. Boujday, *Biosensors* **2019**, *9*, 78.
[31] G. Vitiello, L. Clarizia, W. Abdelraheem, S. Esposito, B. Bonelli, N. Ditaranto, A. Vergara, M. Nadagouda, D. D. Dionysiou, R. Andreozzi, G. Luciani, R. Marotta, *ChemCatChem* **2019**, *11*, 4314.
[32] A. Tyagi, A. Yamamoto, H. Yoshida, *Catal. Sci. Technol.* **2018**, *8*, 6196.
[33] M. T. Islam, H. Jing, T. Yang, E. Zubia, A. G. Goos, R. A. Bernal, C. E. Botez, M. Narayan, C. K. Chan, J. C. Noveron, *J. Environ. Chem. Eng.* **2018**, *6*, 3827.
[34] I. H. Chowdhury, M. Roy, S. Kundu, M. K. Naskar, *J. Phys. Chem. Solids* **2019**, *129*, 329.
[35] G. Mikami, F. Grosu, S. Kawamura, Y. Yoshida, G. Carja, Y. Izumi, *Appl. Catal. B* **2016**, *199*, 260.
[36] D. B. Ingram, S. Linic, *J. Am. Chem. Soc.* **2011**, *133*, 5202.
[37] E. M. Seftel, M. Puscasu, M. Mertens, P. Cool, G. Carja, *Catal. Today* **2015**, *252*, 7.
[38] C. M. Puscasu, E. M. Seftel, M. Mertens, P. Cool, G. Carja, *J. Inorg. Organomet. Polym. Mater.* **2015**, *25*, 259.
[39] E. M. Seftel, E. Popovici, M. Mertens, K. De Witte, G. Van Tendeloo, P. Cool, E. F. Vansant, *Microporous Mesoporous Mater.* **2008**, *113*, 296.
[40] G. Zhang, X. Zhang, Y. Meng, G. Pan, Z. Ni, S. Xia, *Chem. Eng. J.* **2019**, *392*, 123684.
[41] X. Huang, I. H. El-Sayed, X. Yi, M. A. El-Sayed, *J. Photochem. Photobiol. B* **2005**, *81*, 76.
[42] H. He, H. Kang, S. Ma, Y. Bai, X. Yang, *J. Colloid Interface Sci.* **2010**, *343*, 225.
[43] E. Grosu, R. Froidevaux, G. Carja, *Gold Bull.* **2019**, *52*, 87.
[44] D. F. Skrzyńska, J. Ftouni, J. S. Girardon, M. Capron, L. Jalowiecki-Duhamel, J. F. Paul, F. Dumeignil, *ChemSusChem* **2012**, *5*, 2065.
[45] N. Han, B. K. Kaang, W. S. Choi, *Adv. Mater. Interfaces* **2018**, *1801366*, 1.
[46] M. J. Akhtar, M. Ahamed, S. Kumar, M. M. Khan, J. Ahmad, S. A. Alrokayan, *Int. J. Nanomed.* **2012**, *7*, 845.
[47] Z. Xiaofei, L. Wang, X. Xu, X. Lei, S. Xu, F. Zhang, *Am. Inst. Chem. Eng.* **2012**, *58*, 573.
[48] Z. Wang, Q. Zhang, D. Kuehner, A. Ivaskab, L. Niu, *Green Chem.* **2008**, *10*, 907.
[49] F. Cavani, F. Trifirb, A. Vaccari, *Catal. Today* **1991**, *11*, 173.
[50] A. A. A. Ahmed, Z. A. Talib, M. Z. Bin Hussein, *Appl. Clay Sci.* **2012**, *56*, 68.
[51] G. Starukh, O. Rozovik, O. Oranska, *Nanoscale Res. Lett.* **2016**, *11*, 228.
[52] P. Roy Chowdhury, K. G. Bhattacharyya, *Dalton Trans.* **2015**, *44*, 6809.
[53] Z. Yang, Z. Li, X. Lu, F. He, X. Zhu, Y. Ma, R. He, F. Gao, W. Ni, Y. Yi, *Nano-Micro Lett.* **2017**, *9*, 1.
[54] X. Zhao, F. Zhang, S. Xu, D. G. Evans, X. Duan, *Chem. Mater.* **2010**, *22*, 3933.
[55] S. P. Sasikala, T. A. Nibila, K. B. Babitha, A. A. P. Mohamed, A. Solaiappan, *Sustain. Environ. Res.* **2019**, *29*, 1.
[56] F. Li, A. Yuasa, K. Ebie, Y. Azuma, T. Hagishitae, Y. Matsui, *Water Res.* **2002**, *36*, 4592.
[57] S. Wang, M. Li, A. J. Patil, S. Sun, L. Tian, D. Zhang, M. Cao, S. Mann, *J. Mater. Chem. A* **2017**, *5*, 24612.
[58] S. K. Kuk, R. K. Singh, D. H. Nam, R. Singh, J. Lee, C. B. Park, *Angew. Chem. Int. Ed.* **2017**, *56*, 1.
[59] X. Ji, C. Liu, J. Wang, Z. Su, G. Ma, S. Zhang, *J. Mater. Chem. A* **2017**, *5*, 5511.
[60] X. Huang, J. Liu, Q. Yang, Y. Liu, Y. Zhu, T. Li, Y. H. Tsang, X. Zhang, *RSC Adv.* **2016**, *6*, 101974.
[61] H. Song, S. H. Lee, K. Won, J. H. Park, J. K. Kim, H. Lee, S. Moon, D. K. Kim, C. B. Park, *Angew. Chem. Int. Ed.* **2008**, *47*, 1749.
[62] D. Chen, D. Yang, Q. Wang, Z. Jiang, *Ind. Eng. Chem. Res.* **2006**, *45*, 4110.
[63] S. S. Bhoware, K. Y. Kim, J. A. Kim, Q. Wu, K. Jinheung, *J. Phys. Chem. C* **2011**, *115*, 2553.
[64] Y. zi Wang, Z. ping Zhao, R. li Zhou, W. fang Liu, *J. Mol. Catal. B* **2016**, *133*, S188.
[65] S. Kawamura, M. C. Puscasu, Y. Yoshida, Y. Izumi, G. Carja, *Appl. Catal. A* **2015**, *504*, 238.
[66] A. Sánchez-Iglesias, J. Barroso, D. M. Solís, J. M. Taboada, F. Obelleiro, V. Pavlov, A. Chuvilin, M. Grzelczak, *J. Mater. Chem. A* **2013**, *4*, 7045.
[67] R. K. Yadav, J. Baeg, G. H. Oh, N. Park, K. Kong, J. Kim, D. W. Hwang, S. K. Biswas, *J. Am. Chem. Soc.* **2012**, *134*, 11455.
[68] S. H. Lee, J. Ryu, D. H. Nam, C. B. Park, *Chem. Commun.* **2011**, *47*, 4643.
[69] K. Kinastowska, J. Liu, J. M. Tobin, Y. Rakovich, F. Vilela, Z. Xu, W. Bartkowiak, M. Grzelczak, *Appl. Catal. B, Environ.* **2018**, *243*, 686.
[70] Q. Shi, D. Yang, Z. Jiang, J. Li, *J. Mol. Catal. B* **2006**, *43*, 44.
[71] Y. Wu, J. Ward-Bond, D. Li, J. Shi, S. Zhang, Z. Jiang, *ASC Catal.* **2018**, *8*, 5664.
[72] R. K. Yadav, J.-O. Baeg, A. Kumar, K. Kong, G. H. Oh, N.-J. Park, *J. Mater. Chem. A* **2014**, *2*, 5068.
[73] S. Chen, P. Schopfer, *Eur. J. Biochem.* **1999**, *735*, 726.
[74] J. Rocha-Martin, S. Velasco-Lozano, J. M. Guisán, F. López-Gallego, *Green Chem.* **2014**, *16*, 303.

Submitted: June 24, 2021
Accepted: September 29, 2021

FULL PAPERS

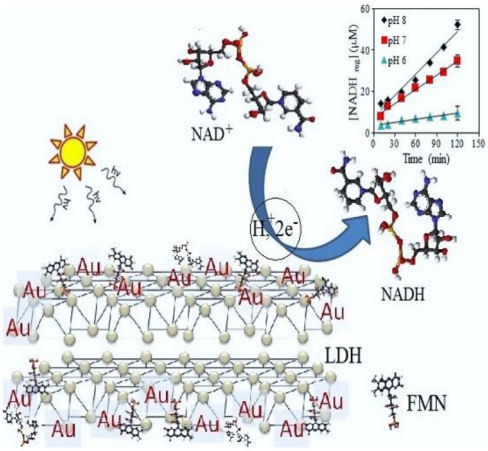

*Dr. E.-F. Grosu, Dr. J.-S. Girardon, Prof. G. Carja, Prof. R. Froidevaux**

In this work, dispersed gold nanoparticles on layered double hydroxide matrix were synthetized via simple and environmental-friendly protocols. The resulted catalyst, AuNPs/ZnAl-LDH, was used for the first time in a cofactor regeneration reaction. The combination between LDH nanomaterial, FMN (flavin mononucleotide) as a mediator, and the solar light was demonstrate to be efficient in photoconverting NAD^+ into 1,4-NADH.